Nitric Oxide (NO) Generation from Heme/Copper Assembly Mediated Nitrite Reductase Activity

Shabnam Hematian, Maxime A. Siegler and Kenneth D. Karlin*

Department of Chemistry, The Johns Hopkins University, Baltimore, Maryland 21218, United States

ELECTRONIC SUPPLEMENTARY MATERIAL

Contents:

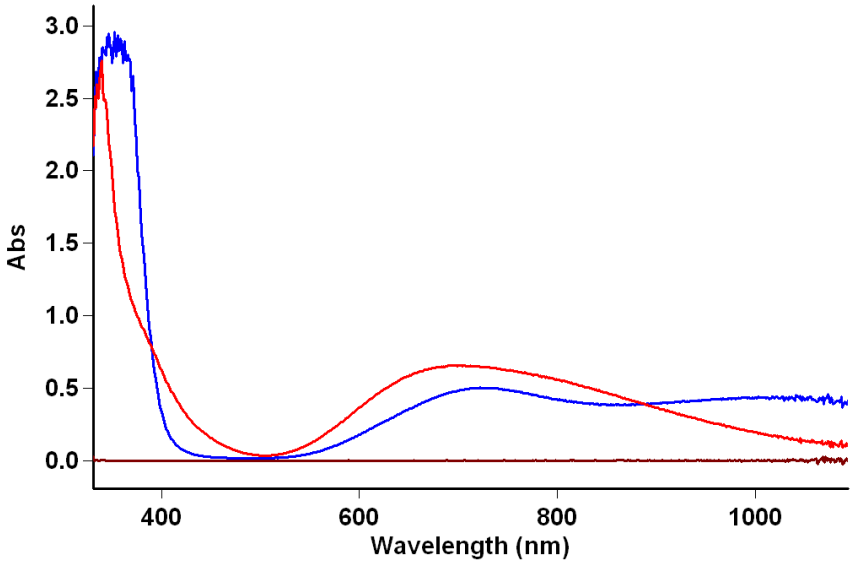

Fig. S1. UV-vis spectra of [(AN)Cu^{II}(Cl)](CF_3SO_3) (blue, λ_{max} = 720 and 1025 nm) and [(AN)Cu^{II}(NO_2)](CF_3SO_3) (red, λ_{max} = 702 nm) 2mM in acetone.

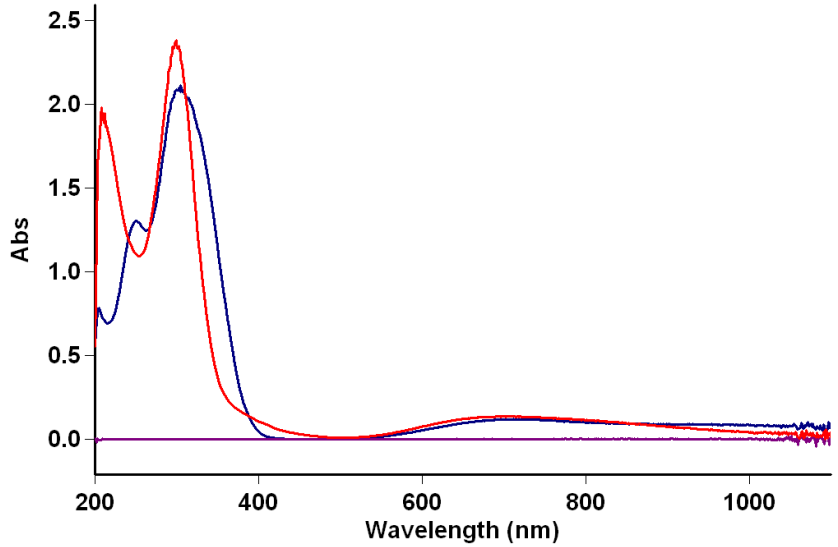

Fig. S2. UV-vis spectra of [(AN)Cu^{II}(Cl)](CF_3SO_3) (blue, λ_{max} = 722 and 1000 nm) and [(AN)Cu^{II}(NO_2)](CF_3SO_3) (red, λ_{max} = 702 nm) 2mM in MeOH.

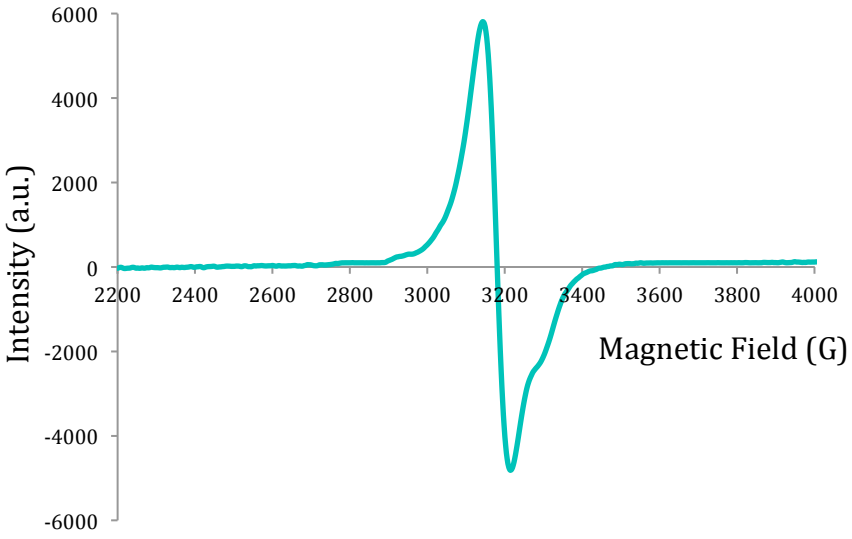

Fig. S3. EPR spectrum of $[(AN)Cu^{II}(Cl)](CF_3SO_3)$ (2mM) in acetone at 22 K.

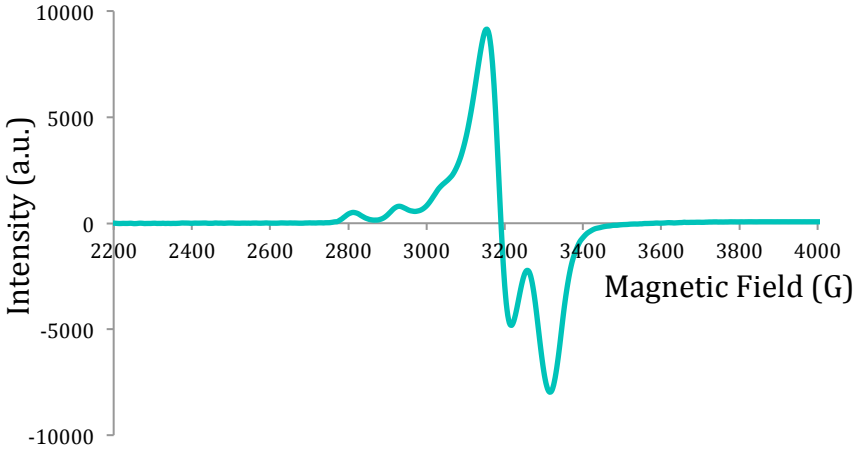

Fig. S4. EPR spectrum of $[(AN)Cu^{II}(Cl)](CF_3SO_3)$ (2mM) in THF:MeCN (4:1) at 15 K.

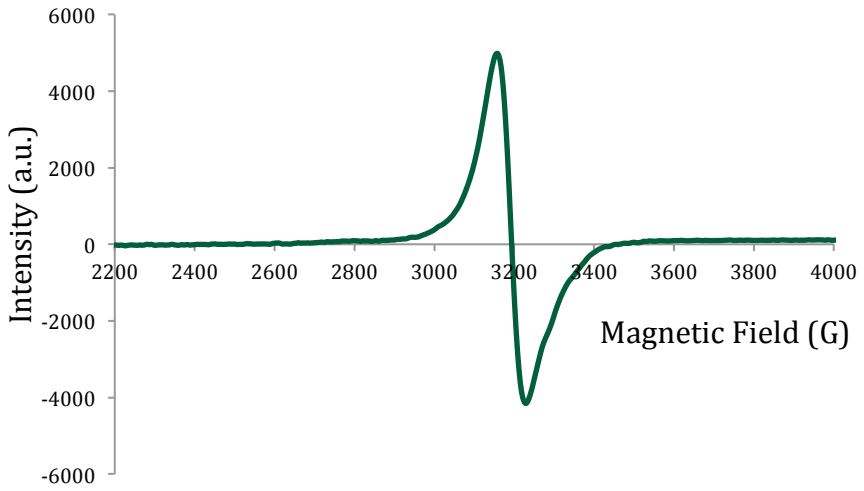

Fig. S5. EPR spectrum of $[(AN)Cu^{II}(NO_2)](CF_3SO_3)$ (2mM) in acetone at 22 K.

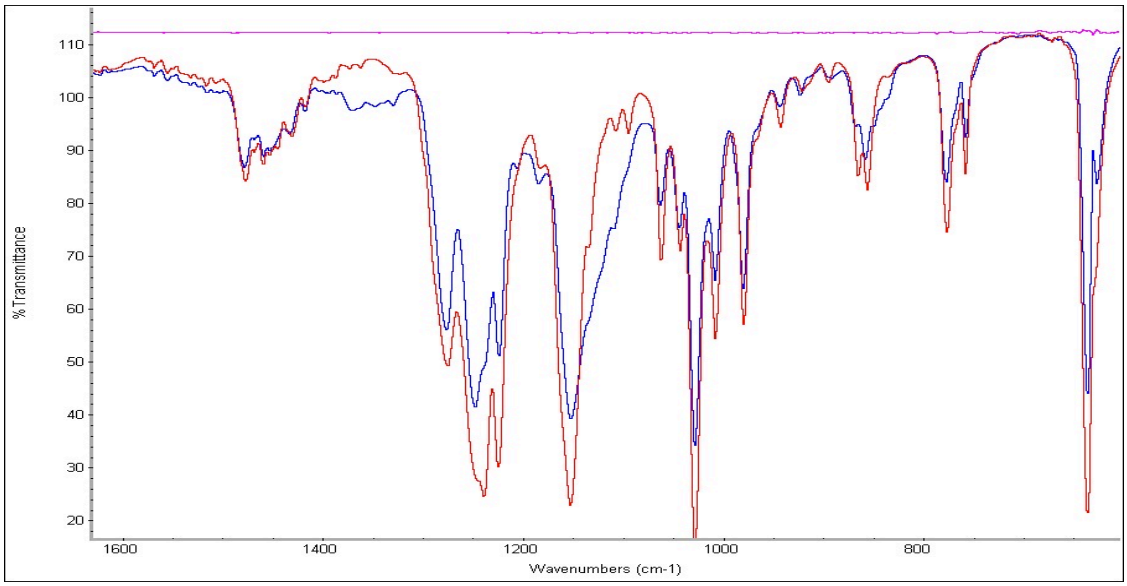

Fig. S6. IR spectra (solid) comparison between the two cupric complexes: $[(AN)Cu^{II}(Cl)](CF_3SO_3)$ (red) $[(AN)Cu^{II}(NO_2)](CF_3SO_3)$ (blue);): $\nu_{as}(NO_2)$ 1370 cm^{-1}, $\nu_s(NO_2)$ 1110 cm^{-1}, and $\delta(NO_2)$ 835 cm^{-1}.

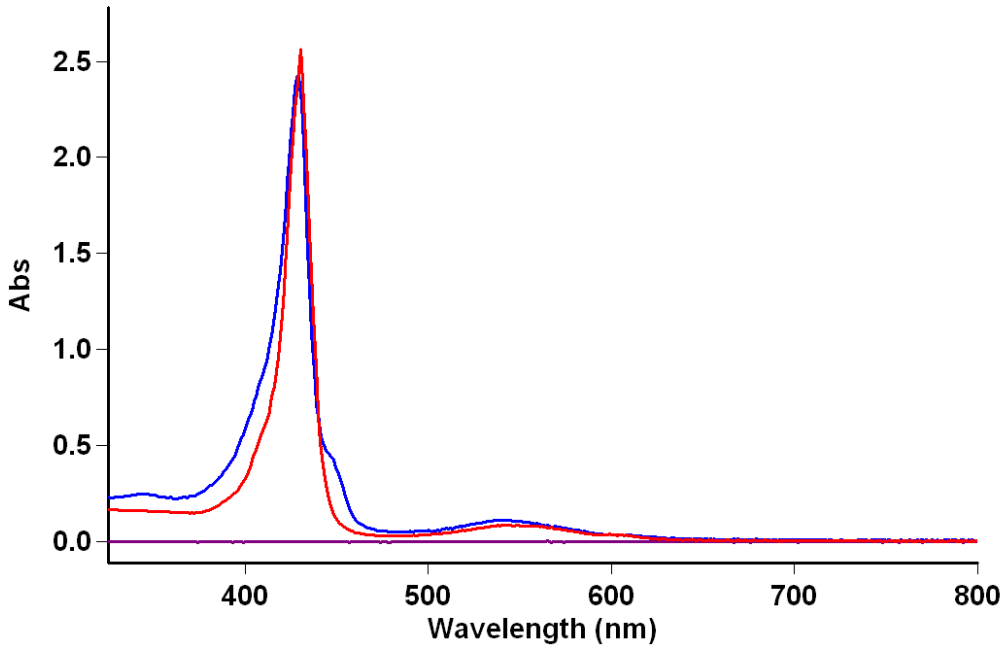

Fig. S7. UV-vis spectra of (TMPP)Fe^{II} (10μM) in acetone (blue, λ_{max} = 429 and 540 nm) and THF (red, λ_{max} = 430 and 542 nm).

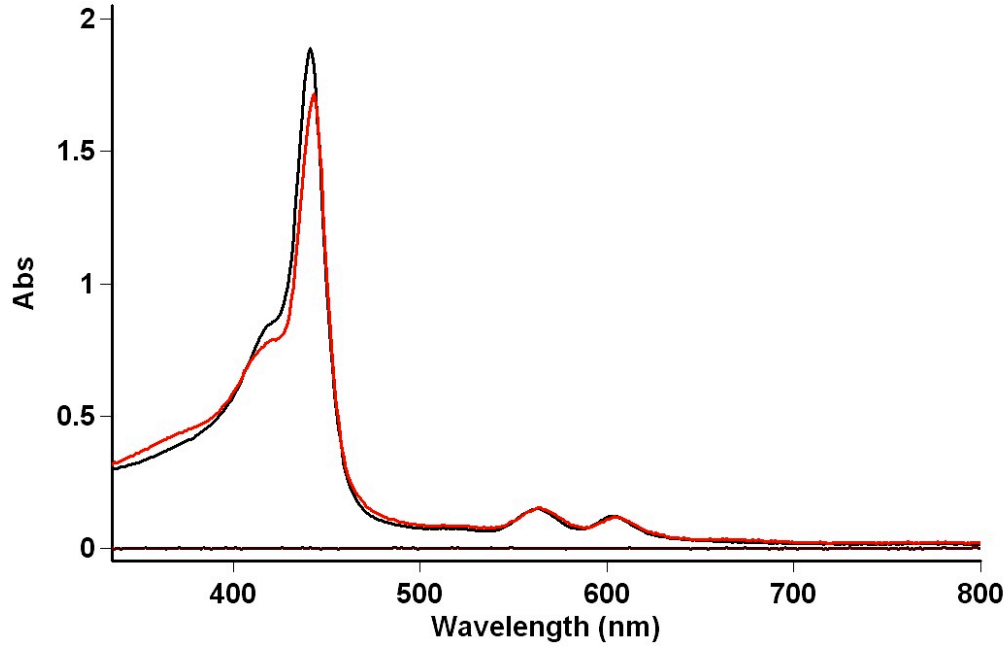

Fig. S8. UV-vis spectra of (TMPP)Fe^{III}-O-Cu^{II}(tmpa)][$B(C_6F_5)_4$] in acetone (7μM) (red, λ_{max} = 443, 564 and 605 nm) and MeCN (10μM) (black, λ_{max} = 441, 561 and 603 nm).

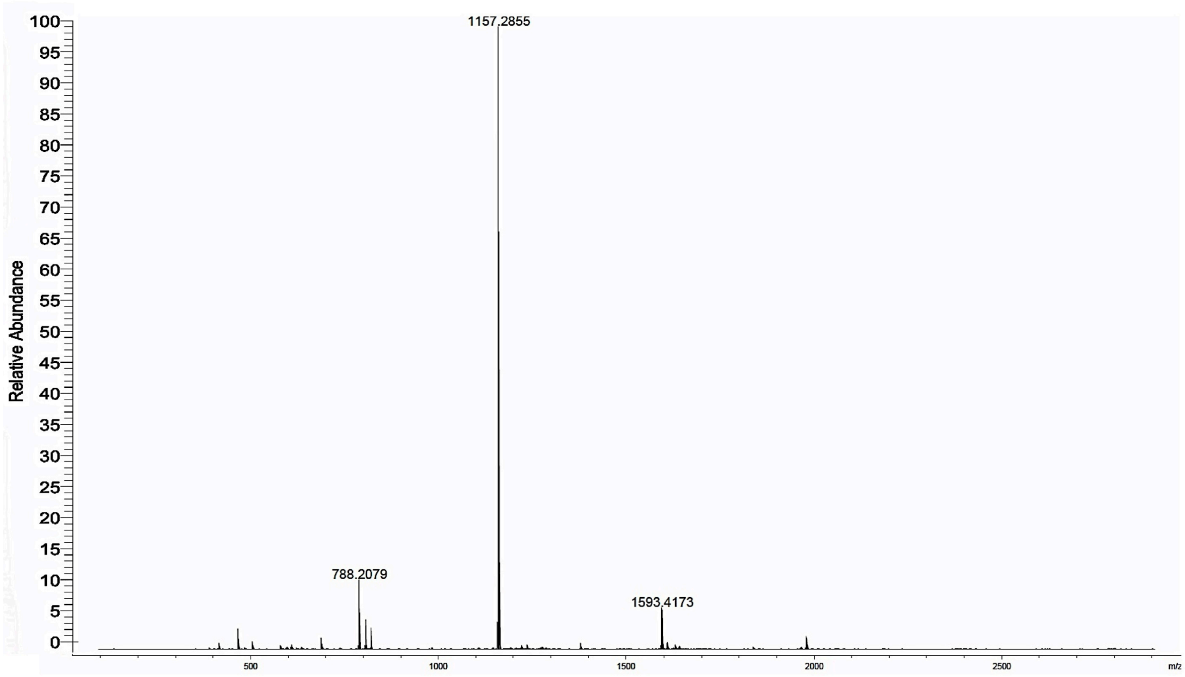

Fig. S9. ESI-MS of (TMPP)Fe^{III}-O-Cu^{II}(tmpa)][$B(C_6F_5)_4$] in acetone: 1157.3 (TMPP)Fe-O-Cu(tmpa); 788.2 (TMPP)Fe; 1593.4 $[(TMPP)Fe]_2O$.

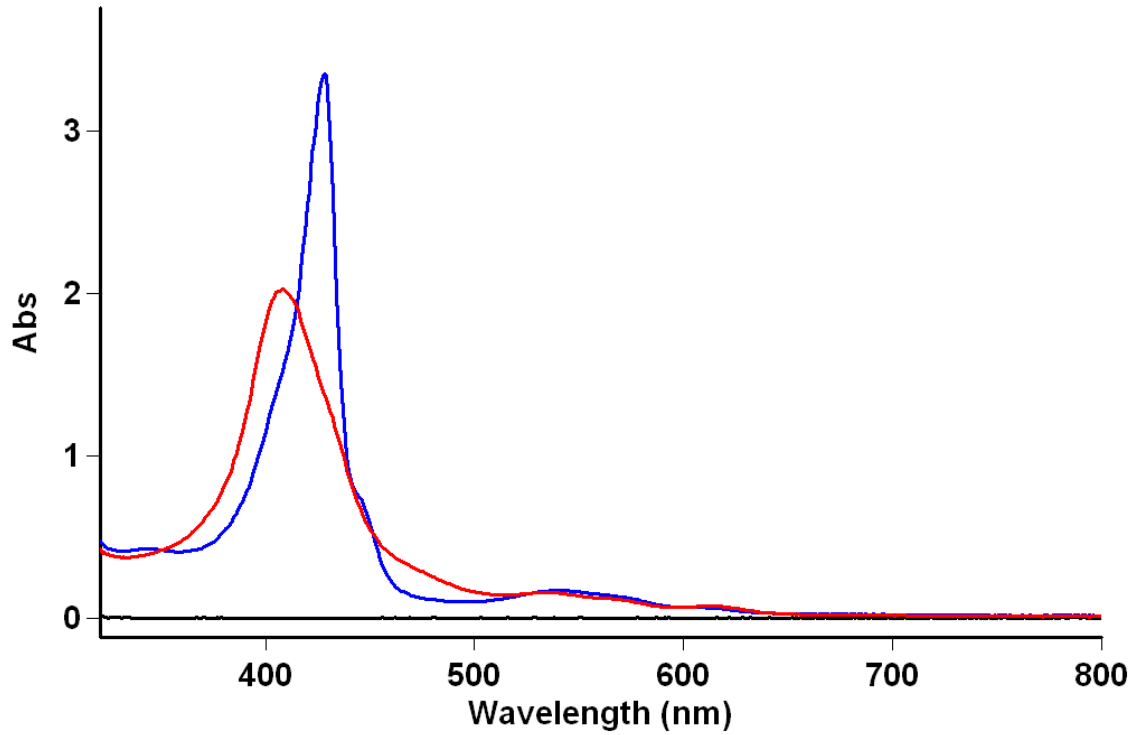

Fig. S10. UV-vis spectra of (TMPP)Fe^{II} in acetone (14μM) (blue, λ_{max} = 429 and 540 nm) and after bubbling excess $NO_{(g)}$ through the solution to form (TMPP)Fe^{II}(NO) (red, λ_{max} = 410, 539 and 614 nm).

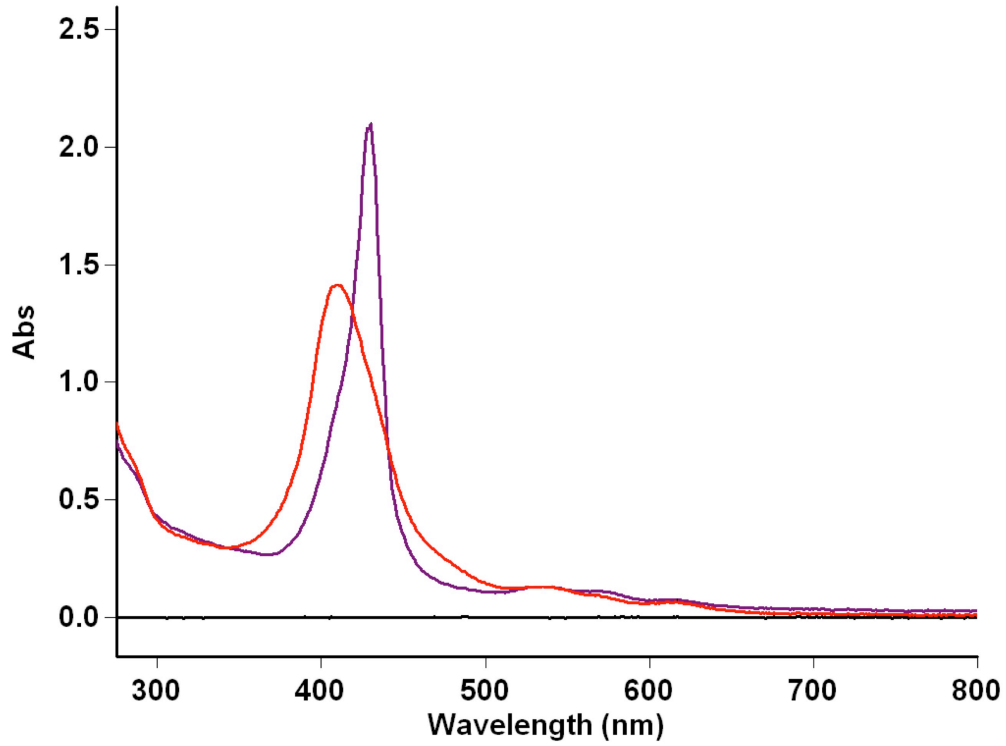

Fig. S11. UV-vis spectra of (TMPP)Fe^{II} in MeCN (10μM) (purple, λ_{max} = 430 and 533 nm) and after bubbling excess $NO_{(g)}$ through the solution to form (TMPP)Fe^{II}(NO) (red, λ_{max} = 410 and 535nm).

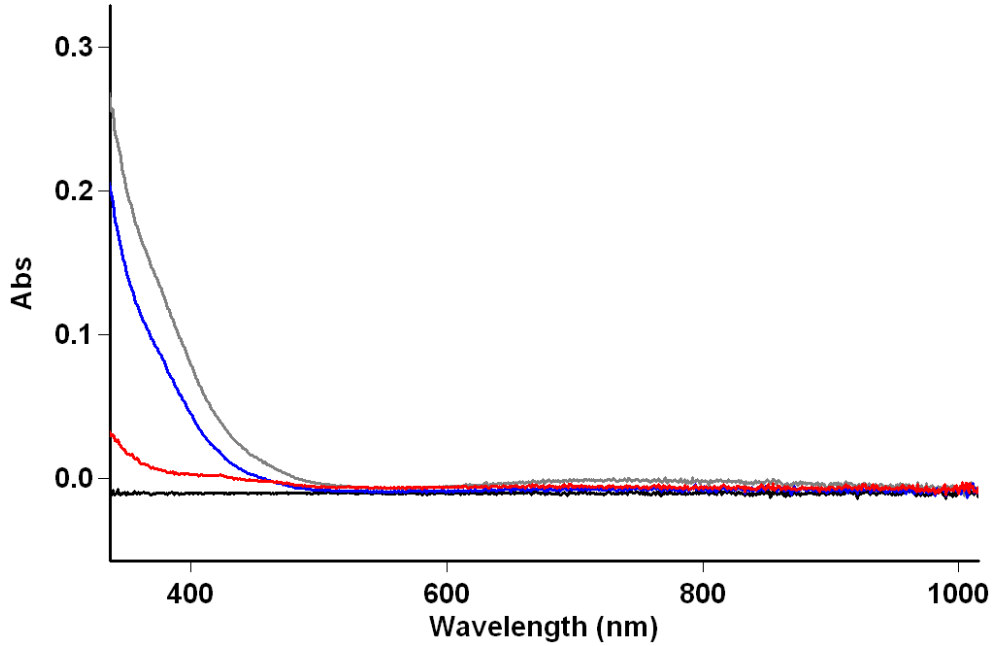

Fig. S12. UV-vis spectra of [(AN)Cu^{I}][$B(C_6F_5)_4$] in acetone (10μM) (red), after addition of 1 equiv of $(Bu)_4N(NO_2)$ (blue) and after stirring overnight (gray).

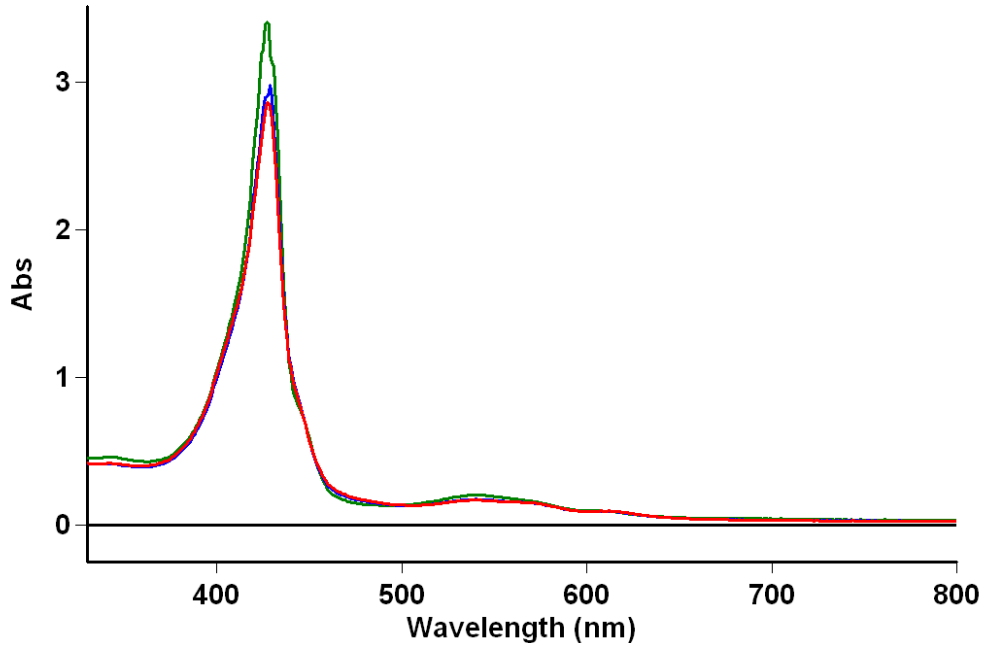

Fig. S13. UV-vis spectra of (TMPP)Fe^{II} in acetone (14μM) (green, λ_{max} = 429 and 540 nm), after addition of 1 equiv of $(Bu)_4N(NO_2)$ (blue) and after stirring for 5 h (red).

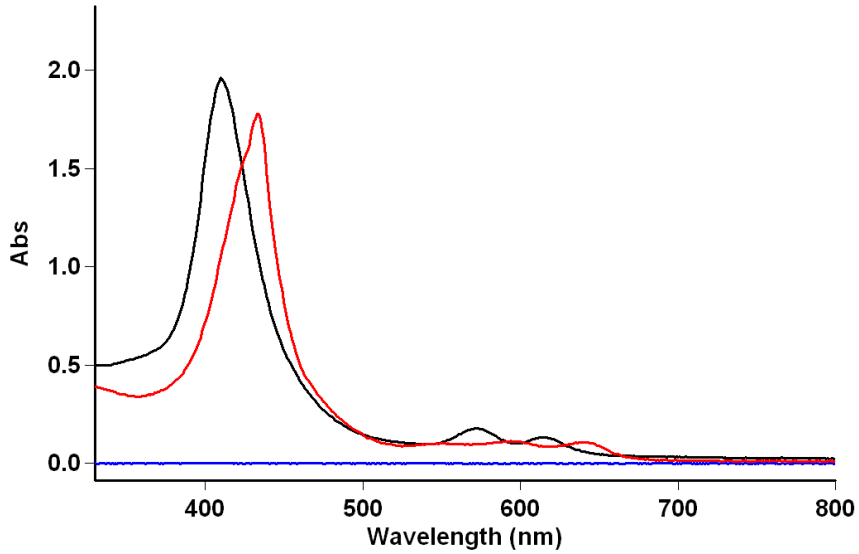

Fig. S14. UV-vis spectra of $[(TMPP)Fe^{III}]_2O$ in acetone (15μM) (black, λ_{max} = 412, 572 and 614 nm) and $[(TMPP)Fe^{III}(OH)]$ in MeCN (10 μM) (red, λ_{max} = 434, 594 and 640 nm). NOTE: To obtain the spectrum of $(TMPP)Fe^{III}(OH)$, we first synthesized $[(TMPP)Fe^{III}(THF)_2](SbF_6)$ via $AgSbF_6$ addition to $(TMPP)Fe^{III}(Cl)$ in THF solvent, for which full experimental details will be presented elsewhere. Then, to a MeCN solution of $[(TMPP)Fe^{III}(THF)_2](SbF_6)$ was added a small excess of tetraethylammonium hydroxide.